Excited States in ^{206}Pb from the Decay of ^{206}Bi

J. C. Manthuruthil

Aerospace Research Laboratories, Wright-Patterson Air Force Base, Ohio 45433

and

D. C. Camp

Lawrence Livermore Laboratory,* University of California, Livermore, California 94550

and

A. V. Ramayya and J. H. Hamilton

Department of Physics and Astronomy,† Vanderbilt University, Nashville, Tennessee 37235

and

J. J. Pinajian

*Isotopes Development Center,‡ Oak Ridge National Laboratory, Oak Ridge, Tennessee 37830,
and Cyclotron and Isotopes Laboratories, N. V. Phillips-Duphar, Petten, North Holland, The Netherlands*

and

J. W. Doornebos

Cyclotron and Isotopes Laboratories, N. V. Phillips-Duphar, Petten, North Holland, The Netherlands

Chemically separated and isotopically separated sources of 6.2-day ^{206}Bi produced by the (p,xn) reactions on lead were used to study the excited states of ^{206}Pb. γ-ray data were taken with a Compton-suppression spectrometer and with a Ge(Li)-Ge(Li) two-parameter analyzer system. From these, 66 γ rays were identified in the decay of ^{206}Bi and 61 of these transitions have been placed from coincidence results, energy sums and differences, and intensity considerations in a decay scheme with 19 excited states. New levels at 2826.4, 2939.6, 3225.5, and 3244.1 keV have been deduced. Spins and parities for all but one excited state were deduced from published internal-conversion electron intensities, relative γ-ray intensities, logft values, and existing angular distribution measurements from particle reactions. The branching ratios, transition multipolarities, and lifetimes for many of the ^{206}Pb levels were calculated by using the wave functions that result from shell-model calculations with phenomenological as well as realistic interactions, and calculations using the two-nucleon random phase approximation.

I. INTRODUCTION

The shell model has been remarkably successful in the description of low-energy nuclear structure in the lead region. During the past few years with the advent of new accelerators and new experimental techniques, many experiments have been performed to test the predictions of the shell model in this region. The results show[1] that there are deviations from simple shell-model predictions. These deviations, however, are not large and most of them can be explained. Many recent experiments have involved charged-particle reactions where cross sections and angular distributions of outgoing particles were measured. The γ-ray decay properties of excited nuclear states are difficult to measure in these high-energy charged-particle reactions. However, the γ-ray decay properties of excited states can be studied

from radioactivities which lead to levels in lead. The γ-ray branching ratios, multipolarity mixing ratios, and transition rates constitute sensitive and detailed tests of the predictions of the shell model. This paper is the first in a continuing study of the decay properties of states in lead nuclei that are accessible from the radioactive decay of bismuth isotopes.

Starting with the well-established single-hole structure[2] of ^{207}Pb, the low-lying levels in ^{206}Pb are a first step towards a more complex structure away from the closed ^{208}Pb core. Theoretical calculations have been done by True and Ford,[3] True,[4] Kuo and Herling,[5] and Vary and Ginocchio.[6] Wave functions have been calculated for excited states in ^{206}Pb by True[4] who used a phenomenological effective interaction and a shell-model space with all possible two-neutron-hole configurations for the six orbitals between $N = 82$

and $N = 126$. The same configuration space was used by Kuo and Herling[5] in their shell-model calculation with various approximations for a realistic effective interaction. Wave functions for ²⁰⁶Pb states have been tabulated and are available for this model. In the Vary-Ginocchio model,[6] the two-nucleon random-phase approximation (2n RPA) with a phenomenological effective interaction is used to calculate the structure of ²⁰⁶Pb. Wave functions for ²⁰⁶Pb states are also available in this model. In Sec. IV, we discuss our results and the properties of the ²⁰⁶Pb states in terms of all three models.

The earliest detailed study of the decay of ²⁰⁶Bi to levels in ²⁰⁶Pb was made by Alburger and Pryce.[7] Using a double-focusing β-ray spectrometer for electron-γ coincidence measurements, and a scintillation spectrometer for γ-ray relative-intensity measurements, they were able to incorporate 28 γ rays into a decay scheme consisting of 12 levels. They also discovered an isomeric state ($J^{\pi} = 7^{-}$) at 2200 keV and measured its half-life to be 145 ± 15 μsec. Later measurements of the internal-conversion coefficients in which the technique of external conversion was used by Stockendal and Hultberg[8] yielded multipolarity assignments in agreement with those given by Alburger and Pryce. For additional references to earlier work on the decay of ²⁰⁶Bi, the reader is referred to the *Table of Isotopes*.[9]

Charged-particle reactions have excited many additional levels. The earliest work is that due to Mukherjee and Cohen[10] who used the ²⁰⁷Pb(d, t)-²⁰⁶Pb reaction to determine the predominant ground-state configuration amplitudes in the wave function for ²⁰⁶Pb. Vallois, Saudinos, and Beer[11] were able to assign a number of l values and spins on the basis of (p, p') angular-distribution measurements. Predominant configuration amplitudes in the wave functions for certain ²⁰⁶Pb states were obtained from the ²⁰⁷Pb(d, t)²⁰⁶Pb reactions[12] and from the excitation function and angular distribution measurements[13] in (p, p') scattering from the isobaric analog states of ²⁰⁷Pb. The (p, t) and (t, p) reactions leading to states in ²⁰⁶Pb have also been carried out.[14,15] The most recent work[16] using the ²⁰⁸Pb(p, t)²⁰⁶Pb reaction studied the two-neutron-hole states in ²⁰⁶Pb and yielded results in good agreement with the shell-model calculations of True[4] and Kuo and Herling.[5]

The previous decay-scheme studies were done with scintillation spectrometers for γ-ray measurements and many uncertainties remained. The present high-resolution γ-ray spectroscopy with Ge(Li) detectors utilizing both singles and coincidence data clears up many of these uncertainties. Our studies along with relative conversion-elec-

tron intensities and logft values have been used to establish J^{π} values for the known ²⁰⁶Pb levels and may even lead to the identification of the static and dynamic properties of the ²⁰⁶Pb nucleus. The detailed γ-ray studies reported here have been successful in both these areas.

II. EXPERIMENTAL PROCEDURES

A. Source Preparations

The 6.24-day ²⁰⁶Bi activity was prepared by irradiating natural lead with 30.5-MeV protons from the Phillips-Duphar cyclotron at Petten, Netherlands. The (p, xn) reaction also produces varying amounts of 11.3-h ²⁰³Bi, 11.3-h ²⁰⁴Bi, and 15.3-day ²⁰⁵Bi plus a negligible amount of 30-yr ²⁰⁷Bi. The target was processed by heating the copper base plate containing the 5-cm-diam 0.3-cm-thick lead target and scraping the lead out. The lead was dissolved in fuming nitric acid and the bismuth precipitated with ammonium hydroxide. The precipitate was isolated by filtration through a glass frit, dissolved in nitric acid, adjusted in pH, and the bismuth activity extracted with dithizone solution. After washing the dithizone free of lead, the solution was evaporated to dryness, treated with nitric acid to destroy the organic residue, and taken up in dilute nitric acid. Adding iron carrier and coprecipitating the bismuth on iron hydroxide several times further reduced solids. The iron was removed by extraction with methyl isobutyl ketone (4-methyl-2-pentanone). The aqueous phase containing the bismuth activity was treated with nitric acid to destroy organic materials and then taken up in dilute hydrochloric acid.

The ²⁰⁶Bi activity was isotopically separated from the other activities using a 160-cm 90° sector laboratory-type isotope separator. An arc/plasma-type ion source was used. The sample, consisting of the bismuth activities with natural bismuth chloride added as carrier, was vaporized out of a tungsten crucible. The yield was 2.5 to 3% with the separated ions collected as a small 5-mm-diam spot on 0.125-mm aluminum foil.

B. γ-Energy and Intensity Measurements

The γ-ray singles spectrum was measured with a 7-cm³ 12-mm depletion depth Ge(Li) detector which was the central detector in a Compton-suppression spectrometer.[17,18] The system consists of the germanium detector housing enclosed by two 22.9-cm-diam by 11.4-cm-thick NaI(Tl) scintillation detector machined to allow maximum enclosure of the Ge(Li) detector. Typical resolutions obtained with this system are 1.0, 2.0,

and 3.0-keV at 122, 1332, and 2754 keV.

The traditional method of measuring standards and unknowns simultaneously was used to determine the energy of the more prominent γ rays in the decay of ^{206}Bi by using a well-stabilized well-calibrated singles Ge(Li) detector system developed by Gunnink *et al.*[19] Efficiency determinations were carried out using standards obtained from International Atomic Energy Agency in Vienna. The sources include ^{241}Am, ^{57}Co, ^{203}Hg, ^{137}Cs, ^{54}Mn, ^{60}Co, and ^{88}Y. The efficiency curve was extended to 2.8 MeV using ^{24}Na. Final errors adopted for the efficiency curve are $\pm 4\%$ from 50 to 200 keV, and $\pm 2\%$ from 200 keV to 3 MeV. Additional details on the methods used in calibrating the detector efficiency can be found in work of Camp and Meredith.[20]

The relative γ-ray intensities were obtained using a computer code entitled SAMPO.[17,21] Essentially, the code uses strong isolated peaks in the spectrum of interest to define a set of peak-shape parameters which through interpolation are applicable over the entire spectral region. These shape parameters contain all the informa-

tion on tailing, energy, and count-rate dependence characteristic of germanium detectors.[22]

Figure 1 shows a CALCOMP plot of the γ-ray spectrum from the decay of ^{206}Bi obtained using one of the isotopically separated sources. Most of the peaks observed are identified. A single- or double-escape peak is denoted by an upper case S or D; while a lower-case d indicates the presence of a doublet. The label CE denotes the presence of a partially suppressed Compton edge associated with a γ ray of medium or weak relative intensity.

Table I lists the energies and relative intensities of the 66 γ rays observed in the decay of ^{206}Bi. The errors on the energy values in the table are determined from calibration standards and the goodness of fit by the computer code. The relative intensities have been normalized to an arbitrary intensity in percent $\times 10^3$ for the 803.10-keV transition. The probable errors shown for the relative intensities include the errors of the relative efficiency curve and a fitting error determined by the computer code used to integrate the peaks.
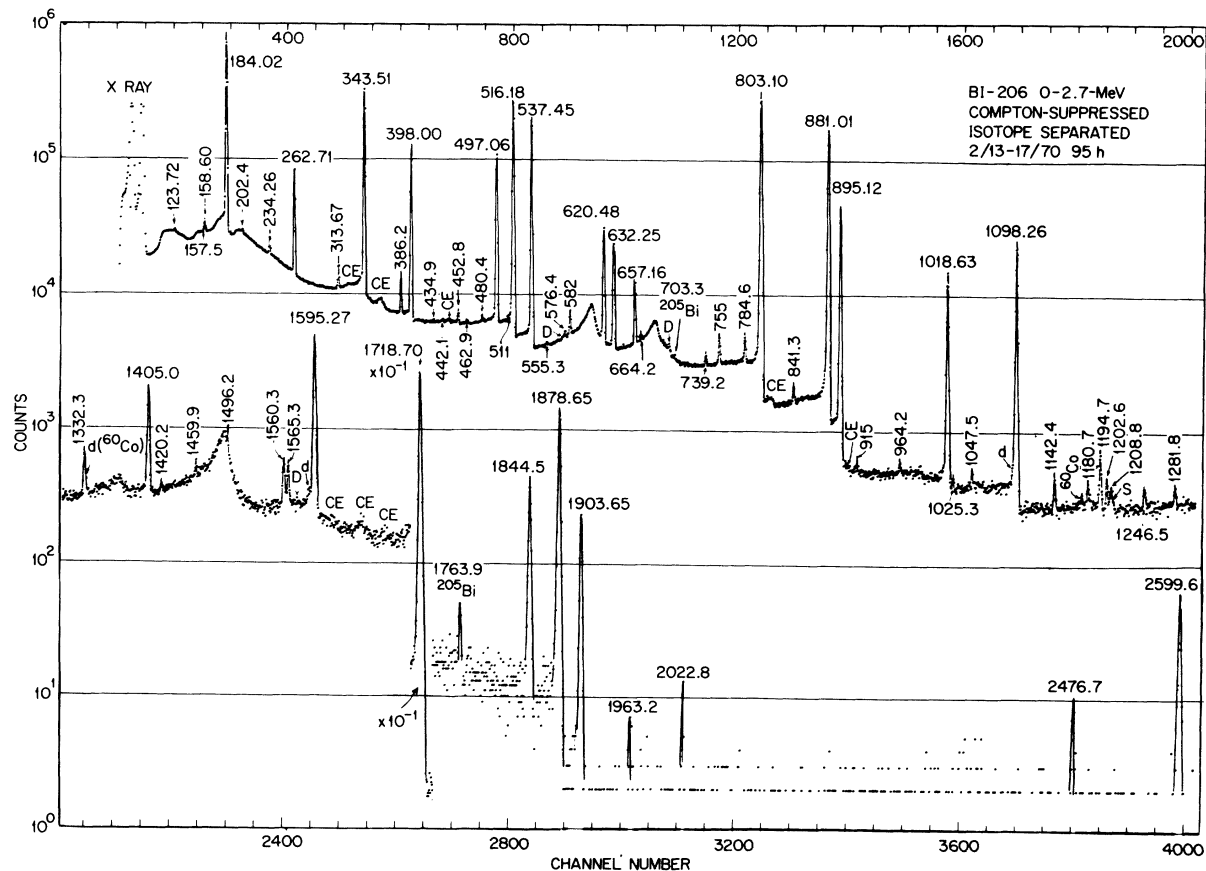
FIG. 1. A Compton-suppressed singles spectrum of isotopically separated ^{206}Bi sample counted for 95 h.

C. γ-γ Coincidence Measurements

The γ-γ coincidence measurements were per-
formed with one of the isotopically separated
^{206}Bi sources using two 35-cm^3 Ge(Li) detectors
coupled to a Nuclear Data 3300 two-parameter
analyzer with dual 4096-channel analog-to-digital
converters. The two germanium detectors were
located at 90° and surrounded by lead cones to
minimize crystal to crystal Compton scattering.
The spectrum from one of the detectors was
stored in 2048 channels so that two 2048-channel
coincidence spectra could be read into the ana-
lyzer memory simultaneously. Digital band-se-
lector gates were set on the background, either
above or just below the photopeaks, as well as on
the photopeak themselves, in order to correct
for Compton-background coincidences. The
source strength and resolving times were such
that chance coincidences could be neglected.

TABLE I. Energies and relative intensities of γ rays
in the ^{206}Bi decay. Asterisk means not placed in decay
scheme.

E_γ	I_γ	E_γ	I_γ
123.63 ± 0.10	23 ± 2	915.00 ± 0.10	31 ± 3
157.52 ± 0.10	36 ± 4	964.22 ± 0.10	37 ± 4
158.60 ± 0.10	83 ± 8	1018.63 ± 0.08	7680 ± 80
184.02 ± 0.03	16 000 ± 300	1025.30 ± 0.10	43 ± 4
202.44 ± 0.10	44 ± 4	1047.55* ± 0.10	57 ± 6
234.26 ± 0.07	244 ± 12	1093.31* ± 0.10	71 ± 7
262.71 ± 0.05	3050 ± 50	1098.26 ± 0.07	13 650 ± 150
313.67 ± 0.07	363 ± 10	1142.37 ± 0.10	112 ± 5
343.51 ± 0.03	23 700 ± 300	1180.70 ± 0.10	67 ± 7
386.20 ± 0.07	522 ± 10	1194.69 ± 0.08	280 ± 15
398.00 ± 0.03	10 860 ± 10	1202.58 ± 0.10	106 ± 6
434.89 ± 0.10	23 ± 2	1208.76* ± 0.10	50 ± 5
442.14 ± 0.10	38 ± 4	1246.46 ± 0.10	85 ± 8
452.84 ± 0.08	158 ± 8	1281.81 ± 0.10	66 ± 7
462.92 ± 0.10	54 ± 5	1332.33 ± 0.10	285 ± 15
480.38 ± 0.10	90 ± 9	1405.01 ± 0.08	1450 ± 25
497.06 ± 0.04	15 480 ± 150	1420.22* ± 0.10	43 ± 4
516.18 ± 0.04	41 200 ± 400	1459.9 ± 0.10	81 ± 8
537.45 ± 0.04	30 750 ± 300	1496.18* ± 0.08	178 ± 10
555.30 ± 0.10	38 ± 4	1560.30 ± 0.08	382 ± 20
576.36 ± 0.10	113 ± 10	1565.34 ± 0.08	307 ± 15
581.97 ± 0.08	490 ± 25	1588.2 ± 0.10	41 ± 4
620.48 ± 0.05	5820 ± 60	1595.27 ± 0.08	5070 ± 60
632.25 ± 0.05	4520 ± 50	1718.70 ± 0.07	32 200 ± 350
657.16 ± 0.05	1930 ± 30	1844.49 ± 0.10	575 ± 25
664.17 ± 0.10	99 ± 5	1878.65 ± 0.08	2030 ± 40
739.24 ± 0.08	159 ± 8	1903.56 ± 0.10	353 ± 15
754.96 ± 0.07	533 ± 10	1963.2 ± 0.30	11 ± 2
784.58 ± 0.07	542 ± 10	2022.8 ± 0.20	13 ± 2
803.10 ± 0.05	100 000	2439.0 ± 0.40	5 ± 2
841.28 ± 0.07	188 ± 9	2476.7 ± 0.20	15 ± 2
881.01 ± 0.05	66 900 ± 700	2599.6 ± 0.20	131 ± 10
895.12 ± 0.05	15 830 ± 160	2759.6 ± 1.0	14 ± 2

Figures 2 and 3 show two coincidence spectra
obtained for the 184- and 881-keV gates. A total
of seven coincidence spectra were analyzed. A
summary of the coincidence relationships is given
in Table II. The entries in the table reflect the
relative strength of the peaks in the spectrum,
compared to the strength of the peaks in the sin-
gles spectrum. A more relevant discussion of
the coincidence results will be given in Sec. III
where the evidence for individual levels is pre-
sented.

D. Internal-Conversion Coefficients

The K conversion coefficients of many transi-
tions were calculated from the relative γ-ray in-
tensities of Table I and the relative conversion-
electron intensities of Kanbe et al.[23] obtained with
a 75-cm double-focusing iron-free spectrometer.
The theoretical $E2$ K conversion coefficient (from
the Hager and Seltzer Tables[24]) of the 803.10-keV
$2^+ \rightarrow 0^+$ transition was used as the standard to
normalize the relative γ-ray and electron intensi-
ties. Table III lists the K conversion coefficients
for 47 transitions determined this way along with
the multipolarity assignments we propose. For
those transitions with energies greater than 1500
keV, multipolarity assignments were based on con-
version-coefficient tables of Sliv and Band.[25]

III. DECAY SCHEME

Based on energy fits, intensities, and γ-γ coin-
cidence relationships, the decay scheme of ^{206}Bi
was constructed and is shown in Fig. 4. In order
to obtain limitations on spins and parities, log ft
values were calculated for each level.

The electron capture and β^+ branching ratios
for various levels in ^{206}Pb have been determined
from the relative γ-ray and conversion-electron
intensities in and out of each level. K-conversion-
electron intensities are available for all the strong
transitions. For the L-, M-, and N-conversion-
electron intensities, theoretical conversion coeffi-
cients consistent with the final adopted decay
scheme were used. Alburger and Pryce[7] showed
that β^+ feeding is extremely small and gave a
limit for this feeding as <0.04%. Therefore, all
the feeding to the ^{206}Pb levels were assumed to
be electron capture. Since the ground state of
^{206}Bi is 6$^+$, and the ground state of ^{206}Pb is 0$^+$,
there is no ground-state β decay. The total elec-
tron-capture intensity is equal to the sum of all
relative total intensities which directly feed the
^{206}Pb ground state, i.e., only the 803.1- and
1459.9-keV transitions. The electron-capture
feeding to each level is the net relative total in-

tensity out divided by the total ground-state feeding. For those levels which are fed very weakly, failure to observe or place one of the weaker transitions would cause a large error in the branching ratio, but would have only a negligible effect on the total electron-capture feeding. Table IV lists the electron-capture energies, the branching ratios in percent and the logft values for all the levels proposed for ^{206}Pb. The logft values were calculated for a decay energy of 3.650 MeV with the aid of the Moszkowski monographs[26] in an expanded version.[9]

In the following paragraphs each level will be discussed separately including, if any, the evidence for spin and parity assignments made.

A. 803.10-keV Level (2⁺)

This level is well established from the γ-ray decay scheme work and also from all the particle-reactions experiments. The spin and parity assignment of 2⁺ for this level is based on internal-conversion-coefficient measurements[7,8] and particle angular-distribution measurements.

B. 1340.55-keV Level (3⁺)

The 537.45-keV γ ray is observed in coincidence with the 803.10-keV γ ray thus establishing the level at 1340.55 keV. Additional evidence for this level comes from the (d, t) and (p, p') work.[12,13] Both groups assign 3⁺ to this level from particle

angular-distribution measurements. The 537.45-keV transition is assigned $M1$ from L-subshell and K-conversion-coefficient measurements. This supports the 3⁺ assignment for this level.

C. 1459.9-keV Level (2⁺)

This level and its spin-parity assignments of 2⁺ are defined by the (d, t), (p, p'), and (p, t) work.[12,13,16] From particle angular-distribution measurements, all three groups have assigned J^π of 2⁺ to this level. In the present work, we observe a 1459.9-keV γ ray which is assigned as a ground-state transition. The 1459.9-keV level is evidently being populated by a 537.86-keV transition from the 1997.76-keV state. The very strong 537.45-keV transition masks this 537.86-keV transition. A 656.8-keV transition is probable from this level to the 803.10-keV level. Unfortunately it is obscured in the singles spectrum by the strong 657.16-keV transition. Similarly in the coincidence gates there is a very strong coincidence between the 657.16-537.45-keV transitions which obscure a possible 656.8-537.8-keV coincidence relationship.

D. 1684.08-keV Level (4⁺)

This level is established from the coincidence results of the 803.10- and 537.45-keV gates. The 881.01-keV γ ray is observed in coincidence with the 803.1-keV transitions and the 343.51-keV γ
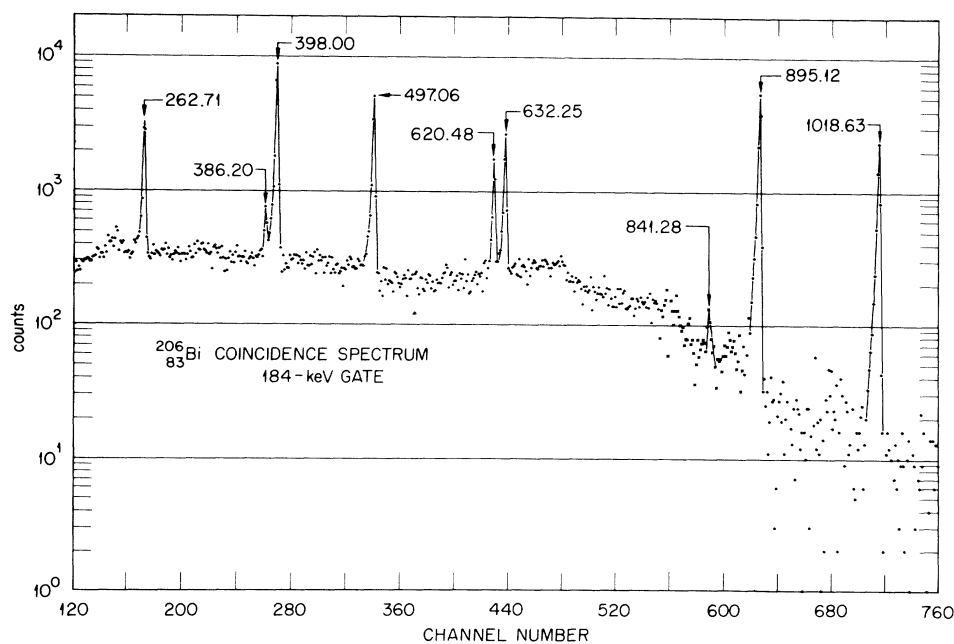
FIG. 2. A portion of the 4096 × 4096-channel coincidence spectrum when the gate was set on the 184-keV γ ray. The contribution from Compton background under the peak is subtracted.

ray is observed in coincidence with the 537.45-keV γ ray, thus establishing the level at 1684.08 keV. The 881.01-keV transition is $E2$ and the 343.51-keV transition is $M1$ from α_K and L-subshell measurements. The parity, therefore, is positive and the spin is most likely 4. Further evidence for a spin and parity of 4^+ comes from the angular-distribution results of (p, p')[11] and (p, t)[16] work.

E. 1997.76-keV Level (4^+)

The 657.16- and the 313.67-keV γ rays are observed in coincidence with the 537.45- and 881.01-keV γ rays, respectively, thus establishing the level at 1997.76 keV. From energy differences and intensity considerations, the 1194.69-keV γ ray was assigned as the decay of this level to the 803.10-keV level. It is probable that a 537.8-keV transition from the 1992.76-keV state feeds the 1459.9-keV level as discussed above. It was not possible to observe it directly, since there is a strong 537.45-keV transition. The 313.67- and 1194.69-keV γ rays are $M1$ and $E2$, respectively, from the K conversion coefficient. In addition the 657.16-keV γ ray is assigned to be $M1$ from
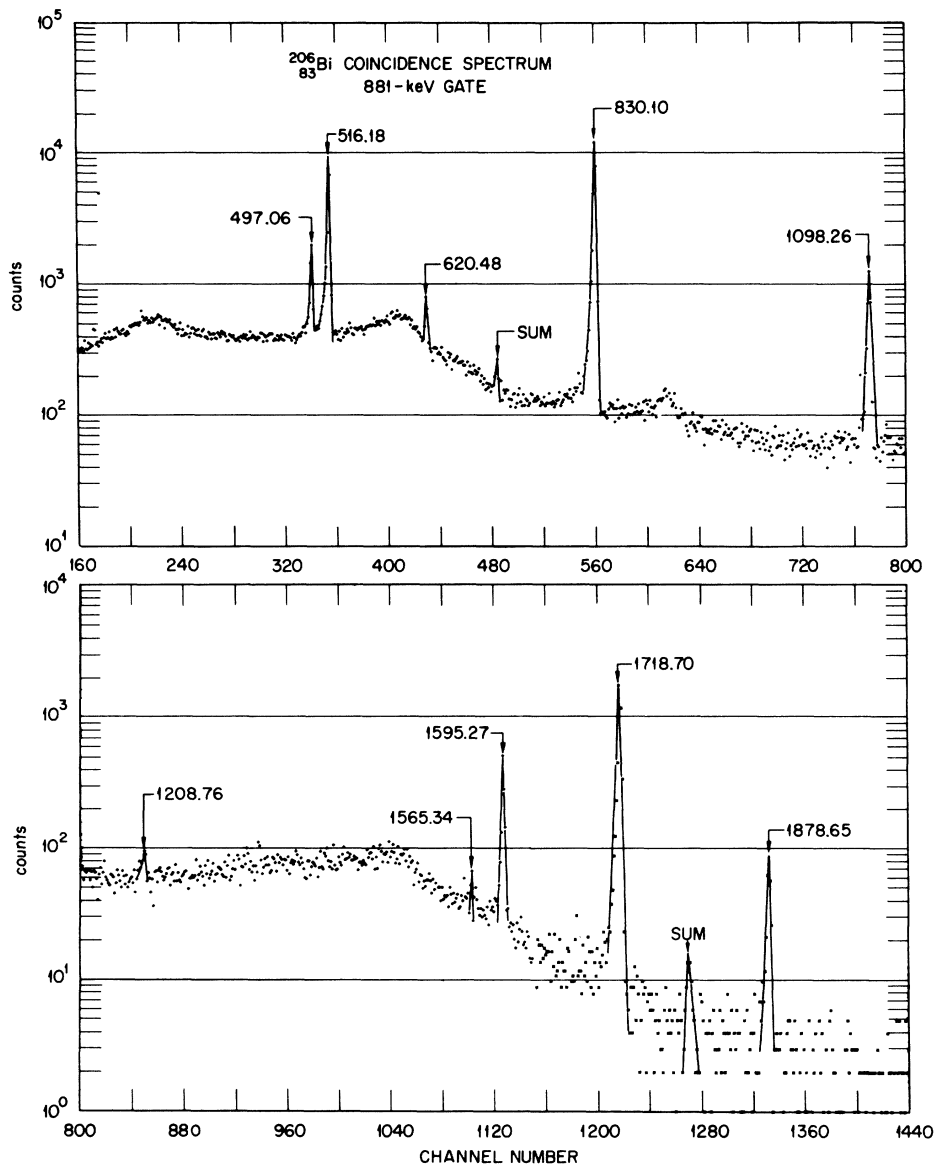
FIG. 3. A portion of the 4096 × 4096-channel coincidence spectrum when the gate was set on the 881-keV γ ray. The contribution from Compton background under the peak is subtracted.

the α_K and L-subshell data. On the basis of these multipolarity assignments, the J^π of this state is uniquely determined to be 4^+. This confirms the assignments of the (p, p')[11] and (p, t)[16] reactions.

F. 2200.23-keV Level (7⁻)

The 516.18-keV γ ray is observed in the 881.01-keV gate thus establishing a level at 2200.23 keV, and thereby confirming the existence of this level known from many of the particle reaction experiments.[10-13,16] The 202.44- and 516.18-keV γ rays are both $E3$ from α_K and L-subshell data. The spin and parity of this level is therefore 7^-. Par-

TABLE II. Coincidence results from the two-parameter γ-γ experiments. The code for the entries is as follows: S=strong; W=weak; N=definitely not in spectrum; all of the coincidence entries are relative to the singles intensities. The γ rays that are not seen in any coincidence spectrum are excluded from the table.

E_γ	Gate						
	184.0	537.5	657.2	803.1	881.0	1098.3	1844.5
157.5						S	
184.0		N	N	N	N	N	
234.3	W					S	
262.7	S				N	S	
313.7						S	
343.5		S		S	N	S	
386.2	S						
398.0	S	N			N	N	
480.4	S						
497.1	S	S	W	S	S	S	
516.2	N	S		S	S	N	
537.5	N	N	S	S	N	S	
620.5	S	W		S	S	S	
632.3	S			N			
657.2	N	S		S			
755.0				W			S
784.6		W	S	W			
803.1	N	S	S	N	S	S	W
841.3	S						
881.0	N			S	N	S	
895.1	S					N	
964.2				W			
1018.6	S				N	N	
1098.3	N	S		S	S	N	
1142.4		W					
1246.5			S				
1281.8			W				
1332.3						W	
1405.0	N	S	S	S			
1560.3						W	
1565.3		W	S				
1595.3	N	S		S	S		
1718.7	N	S		S	S	N	
1844.5	N	N		S	N	N	
1878.7	N	S		S	S	N	
1903.6	N	S		S	N	N	
2599.6		S					

ticle angular-distribution measurements[11-13,16] and inelastic electron scattering measurements[27] confirm the 7^- assignment. A half-life of 126 μsec and a $\log ft$ value of 9.2 are both consistent with the 7^- assignment.

G. 2384.25-keV Level (6⁻)

The coincidence relationship between the 184.02-keV transition and the strong 895.12- and 1018.63-keV γ rays establish this level at 2384.25 keV. Additional evidence comes from (d, t) work[12] where they observe a triton group corresponding to this energy. The strong 184.02-keV γ ray is pure $M1$ from α_K and L-subshell measurements. This restricts the J^π of this state to $(6, 7, 8)^-$. The 895.12- and 1018.63-keV γ rays are both $M1$ from α_K and L-subshell measurements. The 895.12 γ ray deexcites a 5^- level at 3279.32- and the 1018.63-keV γ ray also depopulates another 5^- level at 3402.18 keV (see evidences for these assignments below). This restricts the J^π of the 2384.25-keV level to $(4, 5, 6)^-$. Therefore the spin and parity of this state is 6^-. In addition, the triton angular distribution measurements[12] are consistent with this assignment.

H. 2391.41-keV Level

A probable level at 2391.41 keV is established from the energy sum of the 1588.2- and 434.89-keV γ rays. The 434.89-keV γ ray is postulated to deexcite the 2826.40-keV level rather than the 1588.2-keV γ ray, since that would require the level be at 1238.2 keV. This latter possibility is unlikely, since none of the particle reaction populates such a level. The K conversion coefficients of the 434.89- and 1588.2-keV transitions give inconclusive results (see Table III). The $\log ft$ to this level is $\geqslant 11.02$ and, therefore, the spin of this level is probably less than or equal to 4. It should be emphasized that the evidence for a level at this energy is weak and is based on the energy sums of two weak γ rays.

I. 2647.6-keV Level (3⁻)

The 1844.49-keV γ ray is observed to be in coincidence only with the 803.10-keV γ ray to establish an excited state at 2647.6 keV. This is supported by (p, p') work[11] and inelastic electron scattering work[28] where a level at this energy was observed. The 1844.49-keV γ ray is $E1$ from its α_K and so the J^π of this state $(1, 2, 3)^-$. The 754.96-keV γ ray which decays to this state from the 5^- state at 3402.78 keV is $E2$ in character from α_K measurements and this multipolarity limits the J^π to $(3-7)^-$. Thus, this state can have

TABLE III. K conversion coefficients and multipolarities for certain transitions in ^{206}Pb. All the electron intensities were taken from Ref. 23.

Reference	E_γ (keV)	I_γ	I_K	$\alpha_K \times 10^3$	α_K (Theory) [a] $\times 10^3$ E1	E2	M1	E3	Assignment
b	123.63	23 ± 2	11.5 ± 2.4	4050 ± 1100	209	447	4330		$M1+$ (<1.6% $E2$)
b	157.52	36 ± 4	6.40 ± 1.25	1440 ± 500	115	289	2180		$M1+$ (<3.9% $E2$)
b	158.60	83 ± 8	27.3 ± 1.5	2664 ± 370	113	285	2140		$M1+$ (<2.1% $E2$)
b	184.02	16 000 ± 300	3350 ± 130	1690 ± 100	78	206	1400		$M1+$ (<0.9% $E2$)
b	202.44	44 ± 4	2.25 ± 0.18	414 ± 78	62	165	1070	433	$E3$
b	234.26	244 ± 12	25.3 ± 1.2	840 ± 85	44	117	717		$M1+$ (<3.7% $E2$)
b	262.71	3050 ± 50	208 ± 9	551 ± 35	33	90	522		$M1+$ (<1.2% $E2$)
	313.67	363 ± 10	14.8 ± 0.75	330 ± 27	22	59	322		$M1$
b	343.51	23 700 ± 300	675 ± 27	230 ± 13	18	48	252		$M1+$ (0.8% $E2$)
b	386.20	522 ± 10	11.0 ± 0.5	171 ± 12	14	37	184		$M1+$ (<12% $E2$)
b	398.00	10 860 ± 100	208 ± 8.0	155 ± 5	13	34	170		$M1+$ (<4.8% $E2$)
	434.89	23 ± 2	0.140 ± 0.031	49 ± 17	11	28	134		$M1$, $M1+E2$, $E1+M2$
	442.14	38 ± 4	0.179 ± 0.048	38 ± 16	10	27	128		$E2$, $(M1+E2)$
	452.84	158 ± 8	2.56 ± 0.15	131 ± 15	10	26	120		$M1$
	462.92	54 ± 5	1.07 ± 0.11	160 ± 40	9	25	113		$M1$
	480.38	90 ± 9	1.26 ± 0.09	113 ± 22	8.6	23	103		$M1$
b	497.06	15 480 ± 150	169 ± 7	88 ± 5	8	21	94		$M1+$ (<2.3% $E2$)
b	516.18	41 200 ± 400	242 ± 10	48 ± 2	7.4	19.5	85	49	$E3$
b	537.45	30 750 ± 300	257 ± 10	68 ± 3	6.8	17.9	76		$M1+$ (<2.9% $E2$)
	555.30	38 ± 4	0.190 ± 0.035	41 ± 13	6.4	17	70		$E2$, $(M1+E2)$
	576.36	113 ± 10	0.892 ± 0.052	64 ± 10	5.9	15.5	64		$M1$
b	620.48	5320 ± 60	38.8 ± 1.7	54 ± 3	5.1	13.4	52		$M1+$ (<6.3% $E2$)
b	632.25	4520 ± 50	24.5 ± 1.2	44 ± 3	4.9	12.9	50		$M1+$ (<8.6% $E2$)
b	657.16	1930 ± 30	10.2 ± 0.5	43 ± 3	4.6	11.9	45		$M1+$ (<19% $E2$)
	664.17	99 ± 5	0.540 ± 0.095	44 ± 11	4.5	11.7	44		$M1$
	739.24	159 ± 8	0.622 ± 0.040	32 ± 4	3.7	9.5	33		$M1$
	754.96	533 ± 10	0.571 ± 0.052	8.7 ± 1.0	3.5	9.1	32		$E2$
c, b	803.10	100, 000	100	8.1		8.1			
	841.28	188 ± 9	0.443 ± 0.045	19 ± 3	2.9	7.4	23.9		$M1$, $M1+E2$
b	881.01	66 900 ± 700	55.4 ± 2.4	6.7 ± 0.4	2.6	6.8	21.2		$E2$
b	895.12	15 830 ± 160	34.0 ± 1.5	17.4 ± 1.8	2.6	6.6	20.3		$M1+$ (<13% $E2$)
	915.00	31 ± 3	0.0232 ± 0.0035	6.1 ± 1.6	2.5	6.3	19.2		$E2$
b	1018.63	7680 ± 80	13.5 ± 0.7	14.2 ± 1.0	2.0	5.2	14.6		$M1+$ (<22% $E2$)
	1025.30	43 ± 4	0.076 ± 0.015	14.3 ± 4.6	2.0	5.1	14.4		$M1$
	1098.26	13 650 ± 150	3.60 ± 0.19	2.1 ± 0.2	1.8	4.5	12.0		$E1$
	1142.37	112 ± 5	0.0223 ± 0.0041	1.6 ± 0.4	1.7	4.2	10.9		$E1$
	1194.69	280 ± 15	0.132 ± 0.016	3.8 ± 0.7	1.5	3.9	9.7		$E2$
	1332.33	285 ± 15	0.0533 ± 0.0066	1.5 ± 0.3	1.3	3.2	7.4		$E1$
	1405.01	1450 ± 25	0.249 ± 0.014	1.4 ± 0.2	1.2	2.9	6.5		$E1$
	1588.2	41 ± 4	0.0361 ± 0.0059	7.1 ± 2.1	0.94	2.3	4.8	4.5	$M1$ or $E3$
	1595.27	5070 ± 60	0.654 ± 0.033	1.0 ± 0.1	0.93	2.3	4.7		$E1$
	1718.70	32 200 ± 350	3.12 ± 0.06	0.78 ± 0.05	0.83				$E1$
	1844.49	575 ± 25	0.0507 ± 0.0051	0.71 ± 0.11	0.74				$E1$
	1878.65	2030 ± 40	0.150 ± 0.011	0.60 ± 0.06	0.71				$E1$
	1903.56	353 ± 15	0.0310 ± 0.0058	0.71 ± 0.17	0.70				$E1$
	2022.8	13 ± 2	0.0075 ± 0.0026	4.7 ± 2.7		5.8($M2$)	2.5	2.8	$(M2)$
	2599.6	131 ± 10	0.0229 ± 0.0051	1.4 ± 0.5			1.3	1.7	$(E3)$

[a] All theoretical conversion coefficients below 1500 keV were taken from the tables of Hager and Seltzer. For those above 1500 keV, the tables of Sliv and Band are used.

[b] This indicates that L-subshell measurements have also been performed for this transition and the final multipolarity assignment is based on the α_K and L-subshell results.

[c] The 803.10-keV transition was used for the normalization by assuming it to be pure $E2$ and thus using the theoretical $E2$ conversion coefficient from Hager and Seltzer Tables.

only a 3⁻ assignment. The log *ft* of greater than 9.85 is consistent with this assignment. Thus, we confirm the 3⁻ assignment made for this state from the (p, p')[11] and electron scattering[28] measurements.

The recent (p, t) reaction work[16] also observes a level at 2650 ± 20 keV and assigns a $J^\pi = 9^-$ from triton angular distribution data. It therefore appears that there may be a doublet near 2650 keV.

J. 2782.26-keV Level (5⁻)

The 784.58-keV γ ray is observed in coincidence

with the 657.16-keV γ ray and the 1098.26-keV γ ray is observed in coincidence with the 881.01-keV γ ray to establish a level at 2782.26 keV. The 581.97- and 398.00-keV γ rays are placed from energy considerations. The 398.00-keV transition is $M1$ from α_K and L-subshell measurements. Thus the J^π for this state is limited to $(5, 6, 7)^-$. The 1098.26-keV transition is $E1$ from its α_K to indicate J^π limits of $(3, 4, 5)^-$. Therefore, the spin-parity of this state is 5⁻. The log *ft* value of 8.46 is consistent with this being a first-forbidden nonunique transition. In the (p, t) work,[16] this

FIG. 4. The final adopted decay scheme for ²⁰⁶Pb from this present work.

level is also observed and on the basis of the triton angular-distribution measurements, they also assign 5⁻ to this state.

K. 2826.40-keV Level (4⁻)

The 1142.37-keV γ ray is observed in coincidence with the 881.01-keV γ ray to establish a level at 2826.40 keV. Additional 434.89-, 442.14-, and 2022.8-keV γ rays are assigned to the decay of this level from energy relationships. The multipolarities of the 442.14-keV γ ray which decays to the 2384.25-keV 6⁻ state is predominantly $E2$ and the 1142.37-keV γ ray which decays to the 4⁺ state at 1684.08 keV is $E1$ from α_K data. In addition, the multipolarities of the 452.84-keV γ ray which decays from a 5⁻ state at 3279.32 keV and the 576.36-keV γ ray which decays from another 5⁻ state at 3402.78 keV are both $M1$ from α_K data. A combination of these data restricts the J^π of this state to 4⁻ or 5⁻. The multipolarity of the 2022.8-keV γ ray which decays from this state to the 2⁺ state at 803.10 keV is $M2$ from its α_K and therefore, the J^π of this state is uniquely determined to be 4⁻.

L. 2864.5-keV Level (7⁻)

This level is established by the 480.38-keV transition in the 184.02-keV gate. Transitions of 664.17 and 1180.70 keV can be placed on energy sum relationships. The multipolarities of the 480.38-keV γ ray which decays to the 2384.25-keV

TABLE IV. The electron-capture energies, branching ratios, and logft values for the decay of ^{206}Bi.

E_0 (keV)	EC+β^+ (%)	logft	Level (keV)	J^π
$Q = 3650$	0		0	0⁺
			803.10 ± 0.05	2⁺
			1340.55 ± 0.06	3⁺
			1459.9 ± 0.1	2⁺
			1684.08 ± 0.05	4⁺
1652.2	≤0.20	≥10.3	1997.76 ± 0.05	4⁺
1449.8	≤0.20	≥10.2	2200.23 ± 0.04	7⁻
1265.7	1.68	9.10	2384.25 ± 0.07	6⁻
1258.6	≤0.20	≥10.0	(2391.41 ± 0.07)	
1002.4	≤0.20	≥9.8	2647.6 ± 0.2	3⁻
867.7	3.92	8.44	2782.26 ± 0.05	5⁻
823.6	≤0.20	≥9.7	2826.40 ± 0.10	4⁻
785.5	0.26	9.5	2864.5 ± 0.10	7⁻
710.4	0.26	9.5	2939.60 ± 0.10	6⁻
633.5	≤0.20	≥9.5	3016.45 ± 0.05	5⁻
424.5	0.23	9.1	3225.53 ± 0.05	6⁻, 7⁻
405.9	0.60	8.53	3244.12 ± 0.05	4⁻
370.7	42.23	6.67	3279.32 ± 0.03	5⁻
247.2	48.50	6.25	3402.78 ± 0.03	5⁻
87.3	2.35	6.68	3562.73 ± 0.05	5⁻

6⁻ state and the 664.17-keV γ ray which decays to the 2200.23-keV 7⁻ state are both $M1$ from α_K data, thereby limiting the J^π of this state to 6⁻ or 7⁻. Additional evidence for this level comes from (p, t) work.[16] From their angular-distribution measurement, they assign 7⁻ to this level. The logft value of 9.53 is high for a first-forbidden nonunique transition; however, it does not rule out a 7⁻ assignment.

M. 2939.6-keV Level (6⁻)

This level is established from a weak coincidence at 157.52 keV in the 1098.26-keV gate. Two other γ rays of energy 555.30 and 739.24 keV are assigned from energy fit to depopulate a level at this energy to lower-lying levels. The 462.92-keV γ ray is placed between the well-established level at 3402.78 keV and this level. The α_K value of the 739.24-keV transition to the 7⁻ state at 2200.23 keV makes it $M1$ multipolarity restricting the J^π to 6⁻, 7⁻, or 8⁻. The multipolarity of the 157.52-keV transition decaying to the 2782.26-keV 5⁻ state is $M1$ from α_K and L-subshell measurement. In addition, the 462.92-keV transition decaying to this state from the 3402.78-keV 5⁻ state also has $M1$ multipolarity from α_K data. These facts uniquely determine the J^π of this state to 6⁻. The logft of 9.48 though somewhat high is consistent with a 6⁻ assignment.

A level at 2930 keV has been observed in (d, t)[12] and (p, t) work.[16] On the basis of triton angular distribution measurements both groups assign 4⁺ to this level. This implies a probable doublet, one state with positive parity and the other with negative parity.

N. 3016.45-keV Level (5⁻)

The 234.26-, 632.25-, and 1332.33-keV γ rays are observed in coincidence with the 1098.26-, 184.02-, and 881.01-keV gates, respectively, thus clearly establishing a level at 3016.45 keV. The 234.26- and 632.25-keV γ rays are $M1$ from α_K and L-subshell measurements. In addition the 1332.33-keV γ ray is $E1$ from α_K results. These three multipolarities uniquely define the spin-parity of this state to be 5⁻. Recent (p, t) work[16] is consistent with this 5⁻ assignment.

O. 3225.53-keV Level (6⁻, 7⁻)

This level is established from the coincidence relationship between the 841.28- and 184.02-keV γ rays. The 1025.30-keV γ ray is assigned to decay from this level on the basis of an energy fit. Both the 841.28- and the 1025.30-keV γ rays have $M1$ multipolarity from α_K measurements. This limits the J^π of this state to 6⁻ or 7⁻. The logft

value of 9.07 is consistent with this assignment.

P. 3244.12-keV Level (4⁻)

The 1246.46-, 1560.30-, and 1903.56-keV γ rays are observed in coincidence with the 657.16-, 881.01-, and 537.45-keV gates, respectively, thus establishing this level at 3244.12 keV. The 1903.56-keV γ ray has $E1$ multipolarity from α_K measurements and this limits the J^π of this state

to 2⁻, 3⁻ or 4⁻. The 158.60-keV γ ray which decays from the well-established 5⁻ state at 3402.78 keV has $M1$ multipolarity from α_K and L-subshell measurements. This selects 4⁻ as the J^π of the 3244.12-keV state. The log ft value of this state is ≥ 8.53 which is in agreement with this 4⁻ assignment. Very recently, based on the deuteron angular-distribution measurements of the ^{205}Tl-(^{3}He, d)^{206}Pb reaction at 51 MeV, Seth and Miller[28] also assign 4⁻ to this state.
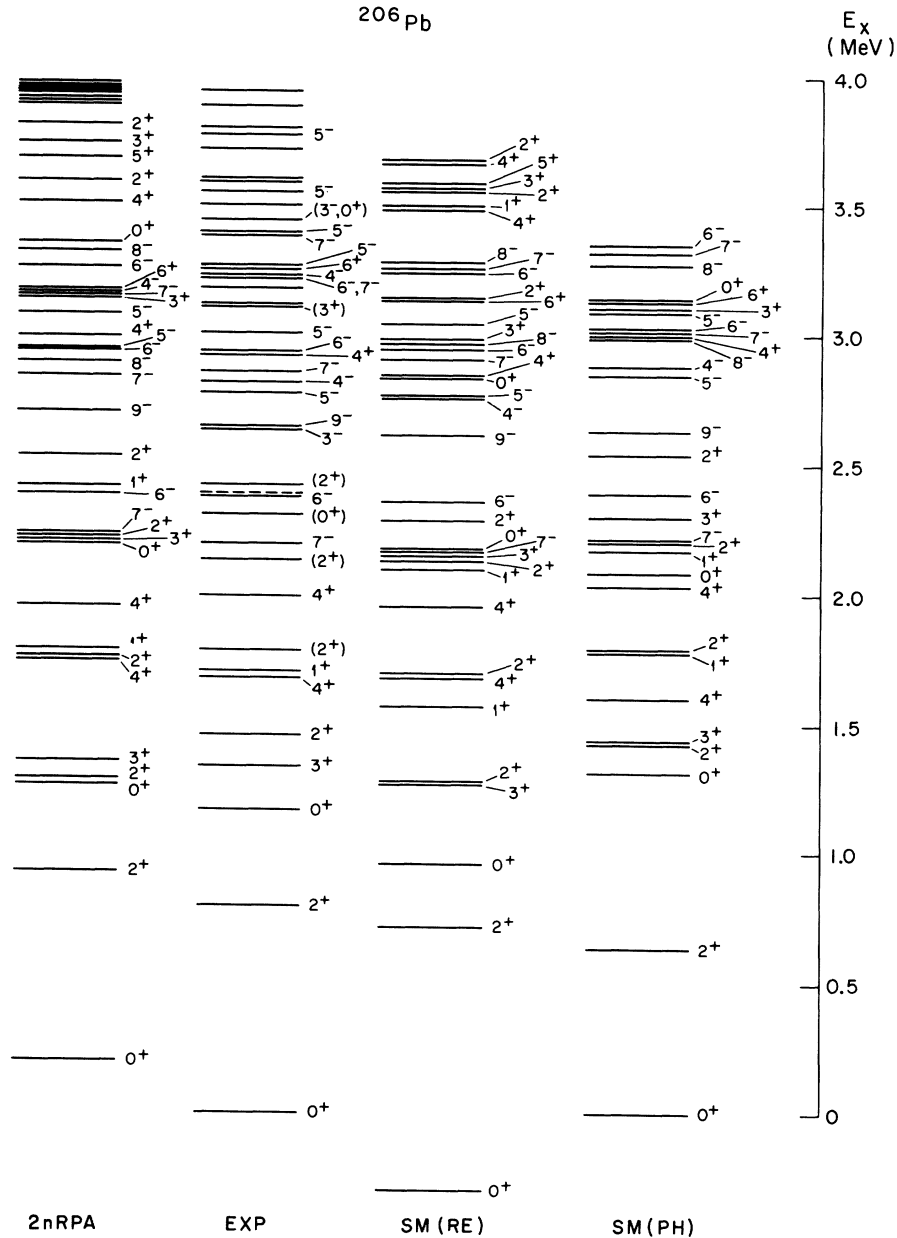
FIG. 5. Comparison of experimental and calculated levels in ^{206}Pb. 2nRPA is a two-nucleon random-phase approximation calculation, SM (RE) is shell-model calculation with realistic interaction, and SM (PH) is shell-model calculation with phenomenological interaction.

TABLE V. Comparison of energies, spins, and parities of levels in ²⁰⁶Pb observed in different experiments. The final adopted values for energies and J^π assignments are given in the last two columns.

(p,p') 1967 (Ref. 11) E	J^π	(p,t),(t,p) 1967 (Ref. 15) E	J^π	(d,t) 1968 (Ref. 12) E	J^π	(p,t) 1968 (Ref. 14) E	J^π	(p,p') 1968 (Ref. 13) E	J^π	(p,t) 1970 (Ref. 16) E	J^π	(β⁺+EC) 1971 E	J^π	Final E	J^π
g.s.	0⁺	g.s.		g.s.	0⁺	g.s.	0⁺	g.s.	0⁺	g.s.	0⁺	g.s.	0⁺	g.s.	0⁺
803±10	2⁺	803		800±10	2⁺	803±50	2⁺	803	2⁺	803±10	2⁺	803.10±0.05	2⁺	803.10±0.05	2⁺
		1165		1170±10	(0⁺)			1150	0⁺	1165±10	0⁺			1168 ±10	0⁺
1328±10		1338		1340±10	(3⁺)			1340	3⁺			1340.55±0.06	3⁺	1340.55±0.06	3⁺
1459±10		1464		1470±10	(2⁺)	1464±50	(2⁺)	1470	2⁺	1464±10	2⁺	1459.9 ±0.10		1459.9 ±0.10	2⁺
		1577												(1577)	
1684±10	4⁺	1682				1682±50	4⁺	1680	4⁺	1682±10	4⁺	1684.08±0.05	4⁺	1684.08±0.05	4⁺
				1710±10	(1⁺)			1710	1⁺					1710 ±10	1⁺
1789±10		1785		1790±10						1785±10	(2⁺)			1788 ±7	(2⁺)
1996±10	4⁺	1997		1990±10	4⁺	1997±50	4⁺			1997±10	4⁺	1997.76±0.05	4⁺	1997.76±0.05	4⁺
		2149		2140±10						2149±10	(2⁺)			2145 ±10	(2⁺)
2199±10	7⁻	2197		2190±10	7⁻	2197±50	7⁻			2197±10	7⁻	2200.23±0.04	7⁻	2200.23±0.04	7⁻
		2314								2314±10	(0⁺)			2314 ±10	(0⁺)
2381±10				2380±10	(6⁻)							2384.25±0.07	6⁻	2384.25±0.07	6⁻
												(2391.41±0.07)		(2391.41±0.07)	
		2421		2420±10						2421±10	(2⁺)			2421 ±10	(2⁺)
2648±10	3⁻	2650										2647.6 ±0.2		2647.6 ±0.2	3⁻
		2653				2650±50	9⁻			2650±10	9⁻			2650 ±10	9⁻
2787±10		2776				2776±50	5⁻			2776±10	5⁻	2782.26±0.05	5⁻	2782.26±0.05	5⁻
		2800										2826.4 ±0.10	4⁻	2826.4 ±0.10	4⁻
										2860±20	7⁻	2864.5 ±0.10	(7⁻)	2864.5 ±0.10	7⁻
2931±10		2924		2930±10	(4⁺)	2924±50	4⁺			2924±10	4⁺			2929 ±10	4⁺
												2939.60±0.10	6⁻	2939.60±0.10	6⁻
3020±10	(5⁻)	3010				3010±50	(5⁻)			3010±10	5⁻	3016.45±0.05	5⁻	3016.45±0.05	5⁻
3124±10		3116		3110±10	(3⁺)									3117 ±10	(3⁺)
		3128												3128 ±10	
		3191								3191±20				3190 ±20	
												3225.53±0.05 6⁻,7⁻		3225.53±0.05	6⁻,7⁻
												3244.12±0.05 4⁻		3244.12±0.05	4⁻
3267±10		3253				3253±50	6⁺			3253±10	6⁺			3253 ±10	6⁺
												3279.32±0.03 5⁻		3279.32±0.03	5⁻
		3383								3390±20	(7⁻)			3390 ±20	(7⁻)

TABLE V *(Continued)*

(p,p') 1967 (Ref. 11) E	J^π	$(p,t),(t,p)$ 1967 (Ref. 15) E	J^π	(d,t) 1968 (Ref. 12) E	J^π	(p,t) 1968 (Ref. 14) E	J^π	(p,p') 1968 (Ref. 13) E	J^π	(p,t) 1970 (Ref. 16) E	J^π	$(\beta^+ + EC)$ 1971 E	J^π	Final E	J^π
3403 ± 10	5^-	3445										3402.78 ± 0.03	5^-	3402.78 ± 0.03	5^-
3453 ± 10	$(3^-, 0^+)$	3511												3453 ± 10	$(3^-, 0^+)$
										3510 ± 20				3510 ± 20	
3560 ± 10	(5^-)	3595										3562.73 ± 0.05	5^-	3562.73 ± 0.05	5^-
		3610								3600 ± 20				3600 ± 20	
														3610	
3721 ± 10														3721 ± 10	5^-
3776 ± 10	5^-	3755								3760 ± 20				3776	
		3805												3805	
										3890 ± 20				3890 ± 20	
										3950 ± 20				3950 ± 20	

Recent (p, t) experiment[16] reports a level at 3253 keV and on the basis of their angular-distribution measurements, they assign 6^+ to this state. Thus there may be a doublet near 3250 keV, since the state seen in (p, t) reaction may not be the one observed in the present work.

Q. 3279.32-keV Level (5⁻)

This level is established on the basis of the following coincidence relationships: (1) The 262.71- and 497.06-keV γ rays are in coincidence with the 1098.26-keV γ ray; (2) the 262.71-, 497.06-, and 895.12-keV γ rays are in coincidence with the 184.02-keV γ ray; (3) the 497.06- and 1281.81-keV γ rays are in coincidence with the 657.16-keV γ ray; and (4) the 497.06- and 1595.27-keV γ rays are in coincidence with the 881.01-keV γ ray. The 452.84- and 2476.7-keV γ rays were placed on the basis of energy fit. The 262.71- and 497.06-keV transitions to two lower-lying 5⁻ levels are both $M1$ multipolarity from α_K and L-subshell measurements. These multipolarities restrict the J^π of this state to 4⁻, 5⁻, or 6⁻. The 895.12-keV transition to the lower-lying 2384.25-keV 6⁻ state is also $M1$ multipolarity from α_K and L-subshell measurements so that J^π is limited to 5⁻ or 6⁻. The 1595.27-keV transition to the 4⁺ state at 1684.08 keV has $E1$ multipolarity from α_K measurements, so the spin and parity of the state is 5⁻. The log ft value of 6.7 is normal for a first-forbidden nonunique transition in agreement with the 5⁻ assignment. The recent ^{205}Tl(^{3}He, d)^{206}Pb reaction[28] work also yields 5⁻ for this state.

R. 3402.78-keV Level (5⁻)

This level is established from the coincidences observed between seven γ rays which decay from this state to lower-lying established levels. An additional five γ rays are assigned to decay from this state on the basis of energy fit. A level at this energy has also been observed in the (p, t) work[16] and (p, p') work.[11] The 123.63-, 386.20-, and 620.48-keV γ rays all decay to lower-lying 5⁻ states and have $M1$ multipolarity from α_K and L-subshell measurements. This limits the J^π of this state to 4⁻, 5⁻, or 6⁻. The 1018.63-keV γ ray which decays to the 6⁻ state at 2384.25 keV also have $M1$ multipolarity from α_K and L-subshell measurements thus limiting the J^π to 5⁻ or 6⁻. The 754.96-keV γ ray which decays to the 3⁻ state at 2647.6 keV is $E2$ or possibly $(M1 + E2)$ in character, thus the J^π is 5⁻. Further confirmation of this assignment comes from the fact that the 1405.01- and 1718.70-keV γ rays, which decay to lower-lying 4⁺ levels, are both $E1$ from α_K results. The log ft value of 6.25 is normal for a

TABLE VI. Comparison between experimental branching ratios, multipolarities, and lifetimes with the predictions of different wave functions sets.

Initial state J^π	Final state	J^π	Experiment Branching ratio	Experiment Multipolarity	Experiment Lifetime (sec)	Vary-Ginocchio (Ref. 6) (2nRPA) Branching ratio	Multipolarity	Lifetime (sec)	Kuo-Herling[a] (Ref. 5) (Shell model real int) Branching ratio	Multipolarity	Lifetime (sec)	True (Ref. 4) (Shell-model phen int) Branching ratio	Multipolarity	Lifetime (sec)
803 2^+	0	0^+	100	E2	$9.0\pm1.0\times10^{-12}$	100	E2	1×10^{-11}	100	E2	1×10^{-11}	100	E2	1×10^{-11}
1341 3^+	803	2^+	100	M1+<2.9% E2		100	M1	1.3×10^{-10}	100	M1	4.2×10^{-11}	100	M1	3.6×10^{-11}
1460 2^+	0	0^+	(100)			13	E2	2.3×10^{-12}	9	E2	3.1×10^{-12}	7	E2	3.5×10^{-12}
	803	2^+				86	M1		90	M1		93	M1	
	1341	3^+				1	M1		0.2	M1		0.3	M1	
1684 4^+	803	2^+	69±1	E2		67	E2	4.9×10^{-12}	54	E2	3.0×10^{-12}	61	E2	3.1×10^{-12}
	1341	3^+	31±1	M1+0.8% E2		33	M1+0.4% E2		46	M1		39	M1	
	1460	2^+	(3)						0.1	E2		0.1	E2	
	1684	4^+	17±1	M1		11	M1		9	M1		14	M1	
2200 7^-	1684	4^+	99.4±0.2	E3	$1.26\pm0.03\times10^{-4}$	99.8	E3	6.9×10^{-4}	100	E3	3.8×10^{-4}	100	E3	2.3×10^{-4}
	1998	4^+	0.6±0.1	E3		0.2	E3		0.04	E3		0.02	E3	
2384 6^-	2200	7^-	100	M1+<0.9% E2	$4.2\pm1.2\times10^{-11}$	100	M1	2.8×10^{-11}	100	M1	5.3×10^{-11}	100	M1	5.3×10^{-11}
2782 5^-	1684[b]	4^+	49±1	E1										
	1998[b]	4^+	2.0±0.2	E1										
	2200	7^-	2.0±0.2	E2		22	E2	$<2.6\times10^{-10}$	0.5	E2	$<1.4\times10^{-12}$	0.5	E2	$<1.4\times10^{-12}$
	2384	6^-	47±1	M1+<4.8% E2		27	M1+44% E2		49	M1		49	M1	
2836 4^-	803	2^+	3±1	M2		5	M2	$<4.0\times10^{-10}$	22	M2	$<2.6\times10^{-10}$	15	M2	$<2.7\times10^{-10}$
	1684[b]	4^+	32±3	E1										
	2384	6^-	13±2	E2, M1+E2		33	E2		38	E2		42	E2	
	2391		8±2											
	2782[c]	5^-	44±5	M1+0.14% E2		31	M1		8	M1		11	M1	
2865 7^-	1684	4^+	26±3											
	2200	7^-	39±2	M1		58	M1+5% E2	3.3×10^{-12}	68	M1+3.5% E2	6.8×10^{-12}	77	M1+9% E2	2.8×10^{-11}
	2384	6^-	35±4	M1		42	M1+0.6% E2		32	M1+1.5% E2		23	M1+11% E2	
2940 6^-	2200	7^-	49±3	M1		58	M1+5.6% E2	3.7×10^{-12}	68	M1+4% E2	6.3×10^{-12}	62	M1+2% E2	2.3×10^{-12}
	2384	6^-	12±2	E2, M1+E2		21	M1+6% E2		10	M1+16% E2		31	M1+1% E2	
	2782	5^-	39±4	M1+<3.9% E2		19	M1		18	M1		6	M1	
	2865	7^-				2	M1		3	M1		1	M1	
3016 5^-	1684	4^+	5±0.3	E1		1	E2	$<2.1\times10^{-13}$	0.4	E2	$<3.2\times10^{-13}$	0.5	E2	$<3.0\times10^{-13}$
	2200	7^-												
	2384	6^-	86±1	M1+<8.6% E2		94	M1		92	M1+0.2% E2		92	M1+0.2% E2	
	2782	5^-	9±1	M1+<3.7% E2		0.1	M1+0.4% E2		2	M1		2	M1	
	2826	4^-							1	M1		0.8	M1	
	2940	6^-							0.1	M1		0.1	M1	

TABLE VI (Continued)

Initial state	J^π	Final state	J^π	Experiment Branching ratio	Experiment Multipolarity	Vary-Ginocchio (Ref. 6) (2nRPA) Lifetime (sec)	Vary-Ginocchio Multipolarity	Vary-Ginocchio Branching ratio	Kuo-Herling[a] (Ref. 5) (Shell model real int) Lifetime (sec)	Kuo-Herling Multipolarity	Kuo-Herling Branching ratio	True (Ref. 4) (Shell-model phen int) Lifetime (sec)	True Multipolarity	True Branching ratio
3226	6⁻	2200	7⁻	18±2	M1	7.1×10⁻¹⁴	M1+1.7% E2	30	7.6×10⁻¹⁴	M1+1.2% E2	32	7.0×10⁻¹⁴	M1+1.1% E2	33
		2384	6⁻	82±4	M1, M1+E2		M1+0.3% E2	69		M1+0.2% E2	66		M1+0.2% E2	64
		2782	5⁻				M1	0.3		M1	2		M1	2.5
		2865	7⁻				M1	0.5		M1	0.5		M1+0.3% E2	0.6
		3016	5⁻				M1	0.6		M1	0.2		M1	0.1

[a] The results presented here were calculated using the wave functions obtained in "approximation 2." (See text for details.)

[b] It is difficult to make comparisons here, since E1 transitions are not allowed in any of the models discussed here (see text for details). Therefore, wherever there is an E1 transition present from a particular level, the theoretical branching ratios given for that level only add up to 100 minus the percentage that go by E1 radiation. Multipolarities and multipole mixings can still be directly compared. Only an upper limit for the lifetime could be given where there is an observed E1 transition.

[c] A transition to the 2782-keV level has been observed by Kanbe *et al.* (Ref. 23) and it is assigned an M1 multipolarity. Total intensity for this transition was calculated by using the electron intensity and assuming the transition to be pure M1.

first-forbidden nonunique transition in agreement with the 5⁻ assignment.

Angular distribution measurements in the (p, p') work[11] also suggest a 5⁻ assignment for this level. However, angular distribution measurements in the recent (p, t) work[16] assign a probable 7⁻ to a state at 3390±20 keV. Therefore, it is not clear whether there are two states here or one.

S. 3562.73-keV Level (5⁻)

The 1565.34- and 1878.65-keV γ rays are observed in coincidence with the 657.16- and 881.01-keV γ rays, respectively, to establish this level at 3562.73 keV. The 915.00- and 2759.6-keV γ rays are assigned to the decay of this level on the basis of energy fit. A level at this energy has also been observed in the (p, p') work.[11] The 1878.65-keV γ-ray transition to the 4⁺ level at 1684.08 keV has E1 multipolarity from α_K results. In addition, the 915.00-keV γ ray which decays to the 2647.6-keV 3⁻ state has E2 multipolarity from α_K data. Thus the J^π of this state is restricted to 3⁻, 4⁻, or 5⁻. The log ft value for the electron-capture decay to this level is 6.68 making the 3⁻ or 4⁻ assignments unlikely. In addition, inelastic proton angular-distribution measurements[11] indicate a 5⁻ assignment for this level. Therefore, this level is most likely 5⁻.

IV. DISCUSSION

In Table V, we have compared the properties of energy levels observed in different experiments. The last two columns contain the synthesis of all the experimental values for energies, spins, and parities for all the states in ²⁰⁶Pb below 3.95-MeV excitation energy.

Several theoretical calculations have been made for the low-lying structure ²⁰⁶Pb. The three latest calculations are compared in some detail with our work. In what follows the excitation energies, decay properties, E1 transitions, and log ft values are discussed separately.

A. Excitation Energies

The earliest shell-model calculation we shall discuss was that done by True[4] who used a phenomenological interaction (hereafter referred to as SMP). A doubly closed ²⁰⁸Pb core was assumed with the two neutron holes distributed over the six available neutron shells ($3p_{1/2}$, $3p_{3/2}$, $2f_{5/2}$, $2f_{7/2}$, $1h_{9/2}$ and $1i_{13/2}$). The results of this calculation are presented in Fig. 5 up to an excitation energy of 3.5 MeV along with the experimental results. The agreement between theory and experiment is reasonably good with the major discrepancy being the inability of the model to predict enough 5⁻, 4⁻,

and 3$^-$ states. There are at least five 5$^-$ states, two 4$^-$ states, and two 3$^-$ states observed below 3.56 MeV, whereas the model predicts two 5$^-$ states, one 4$^-$ state, and one 3$^-$ state. In the extended discussion below of both theoretical and experimental results, it will be evident that these extra states involve more complicated configurations than those retained in a two-neutron-hole shell model. Only a few of the states predicted by the True calculations have not yet been observed experimentally.

The second set of calculations we discuss is the shell-model calculations by Kuo and Herling.[5] In this set of calculations (hereafter referred to as the SMR model), the model space is exactly the same as that used in the SMP model, however, they have used an effective shell-model interaction calculated from a realistic nucleon-nucleon interaction. The effective interaction matrix elements were deduced from the Hamada-Johnston potential according to the model of Kuo and Brown[29] and include the effect of core polarization. The results of this calculation are compared with the experimental data in Fig. 5. [The comparison is for the results of the Kuo-Herling calculation in "approximation 2," where the contribution of (1p-3h) intermediate states are included. A comparison with the results of the calculation in "approximation 3" where the contribution of (2p-4h) intermediate states are also included is slightly worse.] The agreement is good, in fact better than with the SMP model predictions. Comparison of (p, t) spectroscopic factors also gives better agreement with the SMR model.[16] As in the case of SMP model, there are too few 5$^-$, 4$^-$, and 3$^-$ states. The inability of both the SMP and SMR models to predict a sufficient number of 3$^-$, 4$^-$, 5$^-$ states is an indication of an inadequate model space. More negative-parity states might be obtained in this energy region by enlarging the configuration space to include (1p-3h) states in the calculation. Experimentally, these additional negative-parity states decay to many lower-lying levels by $E1$, $M1$, $E2$, $M2$, and $E3$ transitions and therefore, the wave functions could be tested easily by comparing transition rates. On the other hand, it is probably unfeasible to employ a (1p-3h) model space for shell-model calculations in the lead region.

The third set of calculations is that by Vary and Ginocchio[6] where they used the two-nucleon random-phase approximation to calculate the properties of ^{206}Pb (hereafter referred to as 2n RPA model). This model assumes that the low-lying states of ^{206}Pb may be described as correlated two-hole operators (bosons) acting on a correlated ^{208}Pb core. A phenomenological effec-

tive interaction was used to solve for these two-hole modes within the random-phase approximation. The results of this calculation are presented in Fig. 5 along with experimental results. The agreement is good. Again there is an insufficient number of 5$^-$, 4$^-$, and 3$^-$ states below 3.56-MeV excitation energy. However, within the 2nRPA model, these additional states may be understood as two-boson states. That is, these states would be described as the weak coupling of a two-neutron pair-removal boson to a collective p-h boson of the ^{208}Pb core. The 3$^-$ state at 2.648 MeV, the probable 3$^-$ state at 3.453 MeV, the 4$^-$ state at 3.244 MeV, the 5$^-$ states at 3.280, 3.402, and 3.563 MeV are all possible candidates for such two-boson states. The unperturbed energies of some of these states are given in Ref. 6 and they lie close in energy to the observed energies just cited. The mixing with nearby one-boson and three-boson states with the same spin and parity will alter these unperturbed energy eigenvalues as well as their decay properties. A calculation of these two-boson states taking into account the mixing of one-boson and three-boson states would be highly desirable.

B. Decay Properties

From Fig. 5 it is clear that energy eigenvalues, spins, and parities are not sensitive enough to decide which set of wave functions best describe ^{206}Pb. Calculated spectroscopic factors for particle reactions are sensitive to these wave functions; however, a much more sensitive test would be the electromagnetic decay properties of the various levels. Because of this reason, we have calculated[30] the decay properties of ^{206}Pb energy levels for all three sets of wave functions. In these calculations, we have used harmonic-oscillator wave functions. The neutron effective charge was assumed equal to the proton charge. In addition the effective neutron gyromagnetic ratios are taken to be $g_s^{eff} = g_s$ and $g_l^{eff} = 0.13$, where g_s is the bare neutron-spin gyromagnetic ratio. We have also assumed the 2865-keV state to be 7$^-$ and the 3226-keV state to be 6$^-$. We have calculated the branching ratios, multipolarities, mixing ratios, and lifetimes for all three sets of wave functions. The results are presented in Table VI along with the available experimental results. For the SMR model, the results presented are those obtained from the "approximation 2" wave functions . We have also calculated the observables for "approximation 3" and the results are not very much different and therefore, they are not presented here. In the following paragraphs we will discuss the comparison of the decay properties of individual levels with the predictions of the three models.

803-keV level. The only quantity to compare here is the lifetime of this state. All models predict the same lifetime and it is in agreement with experiment.

1341-keV level. Experimentally, the only decay of this state is to the 803-keV level by an $M1$ transition which is in agreement with the predictions of all models. However, the predicted lifetimes are quite different, the 2nRPA model predicts the longest and SMR model predicts the shortest lifetime and therefore an experimental determination would be very useful.

1460-keV level. All three sets of wave functions predict the primary decay to be a transition to the 803-keV level. Experimentally, it is not clear how this level decays. The observed 1459.9-keV γ ray is placed as the decay of this level to the ground state. A possible stronger decay to the 803-keV level could not be observed in the present work due to experimental difficulties (see Sec. III C). Therefore, a proper determination of the decay of this state through some particle reaction is required for a better comparison.

1684-keV level. The agreement for branching ratios are best for 2nRPA model and poor for the SMR model. All models predict the same multipolarities for the transitions and these are in agreement with the experiment. Lifetime predictions are quite different for the three models and a measurement would therefore be very useful.

1998-keV level. The experimental branching ratios are in best agreement with the 2nRPA model calculations. The multipolarities predicted by all models are the same and with the experimental results. It should be noted that SMP model predicts substantially longer lifetime compared to the other two models.

2200-keV level. Again, the experimental branching ratio is in best agreement with the 2nRPA model. The γ-ray multipolarities are in good agreement with all three model predictions. However, there is a substantial discrepancy for the measured and calculated lifetimes for all models. The 2nRPA model gives the worst agreement. One can, in principle, vary the parameters g_s^{eff} and e^{eff} to get better agreement. This does not work, however, as the observed gyromagnetic ratio[31] for this state $(-0.0217 \pm 0.0004)\mu_N$ is quite small. The problem is that one needs an effective charge of 1.9 to account for the half-life, then one needs $g_s^{\text{eff}} = 12.6 g_s$ to obtain the correct gyromagnetic ratio which is unreasonable. The solution[6] to this in the 2nRPA model was found by including a 2% admixture of the two-boson state into this predominantly one-boson state. One can then reproduce the experimental half-life and gyromagnetic ratio with reasonable choices of the param-

eters (see Ref. 6 for further details). A solution to this problem in the shell model could be in the choice of a larger configuration space.

2384-keV state. The experimental branching ratios, multipolarities, and the lifetime are in agreement with the predictions of all three models.

2782-keV state. Experimentally, the main decay of this state is to the 1684-keV state by an $E1$ transition and to the 2384-keV state by an $M1$ transition with weak $E1$ decay to the second 4^+ state and an $E2$ decay to the lowest 7^- state. The absence of $E1$ transitions in all the models is because of the use of a truncated model space (see discussion below regarding $E1$ transitions). If one did not truncate the model space, then only 49% of the intensity is from $M1$ and $E2$ transitions. Because of this, the branching ratios given in the table for all models add up to only 49%. Now, the experimental results are in good agreement with the shell-model predictions. The 2nRPA model predicts the γ-ray multipolarity of the decay to the 6^- state to be $M1 + 44\%$ $E2$, whereas both the shell models predicts pure $M1$ multipolarity in agreement with the experiment. In addition, the 2nRPA model predicts a lifetime which is 2 orders of magnitude longer than the other two-model predictions. A lifetime measurement would be highly desirable in this case. The 2nRPA description of this state appears to be wrong, and it may be that this one-boson state has a small amount of two-boson state mixed into it. The unperturbed energy of the two-boson state is 3.42 MeV which is quite close to this 2.782-MeV state and mixing could very well occur.

2826-keV state. A decay of this state to the 2782-keV state by an $M1$ transition has been observed by Kanbe *et al.*[23] in addition to the transitions reported in the present work. Because of the presence of the $E1$ transition to the 1684-keV 4^+ state, only 68% of the intensity is from $M1$, $M2$, and $E2$ transitions. Therefore the branching ratios given in the table for all models add up only to 68%. The branching ratios appears to be in better agreement with 2nRPA model than with the SMR and SMP models. The multipolarities and lifetimes are approximately the same for all three models.

2865-keV level. The experimental branching ratios are in best agreement with 2nRPA model predictions, however, none of the models predict the observed $E3$ transition to the 1684-keV state. Most likely this is due to the truncated model space we are using rather than due to cancellation. SMP model predicts a lifetime of this state an order to magnitude longer than the other two models and a lifetime measurement would therefore be useful.

2940-keV state. The experimental branching ratios are best agreement with the predictions of 2nRPA model as compared with the other two models. It should be mentioned here that experimentally, it is very difficult to observe the weak branch predicted to the 2865-keV state because of the presence of x rays. The multipolarities and mixing ratios are in agreement with all the model predictions. All models predict approximately the same lifetime for this state. Over all, 2n RPA description appears to be the best for this state.

3016-keV state. The predicted branching ratios for all models are adjusted to 95% because of the presence of the 5% $E1$ transition. The branching ratios are in better agreement with SMR and SMP model when compared to the 2nRPA model. The γ-ray multipolarities are in agreement with experiment for all models. It is perhaps surprising that the model predictions for this state are so close to the experimental results in view of the complicated nearby 5⁻ states. It suggests a high degree of one-boson purity for the 2nRPA model, or, alternatively, it suggests the sufficiency of the two-hole space shell-model description for this state in a region of more complicated states.

3226-keV state. Experimentally, the strongest branch is to the 2384-keV state and the weak branch is to the 2200-keV state. An assumption of $J^{\pi} = 7^{-}$ for this state gives predicted branching ratios for all models in total disagreement with experiment. However, a 6⁻ assumption for this state gives results that are in good agreement with experiment for all models and they are given in Table VI. The agreement is actually very good considering the fact that these models are not expected to work so well for these high-energy states.

For all the models, it is conceivable that agreement could be further improved by varying such quantities as e^{eff}, g_s^{eff}, and g_l^{eff}. We have not done this and we have used values for these parameters which gave best agreement with the properties of the 7⁻ state at 2200 keV and the 2⁺ state at 803 keV. It should be mentioned that agreement with experiment could also be improved by including small admixtures of two-boson states into the one-boson state in the 2nRPA model and analogously including (1p-3h) contributions into the two-hole states in both the shell models.

We have not discussed here the $M1$ transition from the 1.7-MeV 1⁺ state, since that has been recently discussed in a series of papers.[32-34]

C. $E1$ Transitions

In the SMR and SMP models, $E1$ transitions are not allowed due to the choice of the configuration

space. For the six orbitals that are included, the $E1$ transition must involve the $i_{13/2}$ orbital and anyone of the other five orbitals. The highest available orbital is the $h_{9/2}$ orbital and a transition would require carrying off more than one unit of angular momentum, and hence $E1$ transitions are not allowed. Since $E1$ transitions are actually observed, this points to the inadequacy of the configuration space. One can get $E1$ transitions by enlarging the configuration space. For example, $E1$ transitions can take place between (1p-3h) states and two-hole states. Therefore, the shell-model description of those states which decay by $E1$ transitions needs to be revised and improved.

Even in the 2nRPA model, that is with ground-state correlations, $E1$ transitions are not allowed. Again this is a result of model space considerations. In the 2nRPA, electromagnetic transitions involve contributions of the same nature as in the shell-model case plus additional contributions due to amplitudes reflecting ground-state correlations in the ^{208}Pb core. The first type parallels the shell-model case and thus does not contribute to $E1$ transitions. For the second type, the two-neutron-hole-correlation amplitudes are in the model space of single-particle states above the ^{208}Pb Fermi surface, namely, $2g_{9/2}$, $1i_{11/2}$, $1j_{15/2}$, $3d_{5/2}$, $4s_{1/2}$, $2g_{7/2}$, and $3d_{3/2}$, and $E1$ transition would involve the $1j_{15/2}$ and one of the other orbitals. The highest available orbital is the $1i_{11/2}$ orbital and a transition would require carrying off more than one unit of angular momentum, and hence $E1$ transitions are not allowed. $E1$ transitions could go by having some octupole admixture (e.g., small part of the octupole 3⁻ state coupled to the 2⁺ state) in the two-hole states.

D. Logft Values

The ground state of ^{206}Bi is 6⁺ and, therefore, the β decay to the 5⁻, 6⁻, and 7⁻ states in ^{206}Pb are to be classified as first forbidden nonunique. The normal logft values for this type of decay range from 5 to 7. However, the observed logft values to all states in ^{206}Pb are considerably higher (>9) except to three high-lying 5⁻ states at 3.279, 3.403, and 3.563 MeV, and these are the states that are not predicted in any of the models discussed here. These observed large logft values may be qualitatively understood in the following way. For ^{206}Bi, the most probable configuration is $h_{9/2}$ proton coupled to three holes distributed over the six shells $1h_{9/2}$, $2f_{7/2}$, $1i_{13/2}$, $3p_{3/2}$, $2f_{5/2}$, and $3p_{3/2}$, giving a resultant spin and parity of 6⁺. We therefore have configurations of the type $(1h_{9/2}{}^{+}2f_{5/2}{}^{-3})$, $(1h_{9/2}{}^{+}3p_{1/2}{}^{-2}2f_{5/2}{}^{-1})$, $(1h_{9/2}{}^{+}3p_{3/2}{}^{-3})$, etc. The simple shell-model-type 5⁻, 6⁻, and 7⁻ states in ^{206}Pb have the predomi-

nant configurations $(3p_{1/2}1i_{13/2})$, $(2f_{5/2}1i_{13/2})$, and $(3p_{3/2}1i_{13/2})$. β decay can now be retarded for two reasons. First, for β decay to take place, the $h_{9/2}$ proton has to change to a $i_{13/2}$ neutron. This requires that $\Delta J = 2$ and therefore the scalar and vector (rank 0 and rank 1) matrix elements which contribute to the first-forbidden nonunique β decay are not allowed. We can therefore expect retarded β transitions and thus large $\log ft$ values. An example[35] of this type is the β decay of ^{124}Sb where the β decay is from a 3⁻ to a 2⁺ state which is first forbidden nonunique, yet the observed $\log ft$ value is 10.2. The β-decay hindrance was explained[35] there by noting that an $h_{11/2}$ neutron has to change to a $g_{7/2}$ proton and therefore $\Delta J = 2$, and hence a large $\log ft$ value. Second, let us for the moment assume the predominant configuration of the ^{206}Bi ground state to be $(1h_{9/2}{}^{+1}3p_{3/2}{}^{-2}2f_{5/2}{}^{-1})$ and that the β decay is to take place to a state in ^{206}Pb which has the configuration $(3p_{3/2}1i_{13/12})$. Here the β decay is strictly forbidden, since two particles will have to change orbitals for the β decay to proceed. One or the other of the above reasons or a combination of the two are probably the reasons for the large $\log ft$ values.

β decay still proceeds through small components in the wave functions of the parent ^{206}Bi state to components in ^{206}Pb states where an allowed β decay can take place. A quantitative calculation would require a much better knowledge of ^{206}Bi ground-state wave function than presently available. The calculated $\log ft$ values are going to be very sensitive to the amplitudes of the configurations which allows β decay to proceed and as such will be a good test of the wave function.

The observed $\log ft$ values to the three 5⁻ states at 3279, 3403, and 3563 keV are between 6 and 7 which is quite normal for a first-forbidden nonunique β decay. This indicates a good overlap between these three 5⁻ states and the ^{206}Bi ground state. In particular it tends to confirm a 1p-3h or two-boson nature for these states. As an example, these states could have configurations of the type $g_{9/2}{}^{+1}f_{5/2}{}^{-1}p_{3/2}{}^{-2}$ or others.

The β-decay retardation discussed here should also be true for other bismuth nuclei that decay to lead nuclei. Indeed this is true as can be seen in the case of the decay[36] of ^{205}Bi.

V. CONCLUSION

The present level scheme represents a considerable advancement over what is available in the literature. The level structure shown in Fig. 4 includes several new levels, new decay scheme for levels, and new spin and parity assignments. These results were compared with the older shell-model calculations using phenomenological interaction, the recent shell-model calculations using realistic interaction, and the still more recent two-nucleon random-phase-approximation calculations. Comparison of energy eigenvalues, spins, parities, and decay properties showed that the two shell models gave better agreement for energy eigenvalues, whereas 2nRPA model gave better agreement for transition rates. These comparisons suggests new experiments such as lifetime measurements and branching ratio determinations. The model predictions are given for these as yet unmeasured quantities. These measurements could further test the wave functions obtained from the different models. Additional theoretical work to account for the other observed negative-parity states, the experimentally observed $E1$ transitions, and the large $\log ft$ values would be valuable. We have given a qualitative explanation for the hindrance of β decay.

Finally, we note that a new shell-model calculation by Ma and True has been reported.[37] This calculation uses the same model space as that used in the True calculation,[4] however, they have added a small P_3 force to the residual interaction. They obtain an improved ground-state wave function, otherwise, the results for energy eigenvalues, spins, parities, and decay properties are essentially the same as that obtained in the True model.

ACKNOWLEDGMENTS

---

[1]For a summary of recent developments in nuclear spectroscopy in the lead region, see N. Stein, in *Proceedings of the International Conference on Properties of Nuclear States, Montréal, Canada, 1969*, edited by M. Harvey *et al.* (Presses de l'Université de Montréal, Montréal, Canada, 1969), p. 337.

[2]G. Muehllehner, A. S. Poltorak, W. C. Parkinson, and R. M. Bassel, Phys. Rev. 159, 1039 (1967).

[3]W. W. True and K. W. Ford, Phys. Rev. 109, 1675 (1958).

[4]W. W. True, Phys. Rev. 168, 1388 (1968).

[5]T. T. S. Kuo and G. Herling, Naval Research Laboratory Report No. 2258 (unpublished).

[6]J. Vary and J. N. Ginocchio, Nucl. Phys. A166, 479 (1971).

[7]D. E. Alburger and M. H. L. Pryce, Phys. Rev. 95, 1482 (1954).

[8]R. Stockendal and S. Hultberg, Arkiv Fysik 15, 33 (1959).

[9]C. M. Lederer, J. M. Hollander, and I. Perlman, Table of Isotopes (Wiley, New York, 1967).

[10]P. Mukherjee and B. L. Cohen, Phys. Rev. 127, 1284 (1962).

[11]G. Vallois, J. Saudinos, and O. Beer, Phys. Letters 24B, 512 (1967).

[12]R. Tickle and J. Bardwick, Phys. Rev. 166, 1167 (1968).

[13]P. Richard, N. Stein, C. D. Kavaloski, and J. S. Lilley, Phys. Rev. 171, 1308 (1968).

[14]S. M. Smith, C. Moazed, A. M. Bernstein, and P. G. Roos, Phys. Rev. 169, 951 (1968).

[15]E. R. Flynn, G. J. Igo, R. Woods, P. D. Barnes, and N. K. Glendenning, Phys. Rev. Letters 19, 798 (1967).

[16]S. M. Smith, P. G. Roos, A. M. Bernstein, and C. Moazed, Nucl. Phys. A158, 497 (1970).

[17]D. C. Camp, Nucl. Phys. A121, 561 (1968).

[18]D. C. Camp, in Radioactivity in Nuclear Spectroscopy, edited by J. H. Hamilton and J. C. Manthuruthil (Gordon and Breach, New York, 1972).

[19]R. Gunnink, R. A. Meyer, J. B. Niday, and R. P. Anderson, Nucl. Inst. Methods 65, 26 (1968).

[20]D. C. Camp and G. L. Meredith, Nucl. Phys. A166, 349 (1971).

[21]J. T. Routti and S. G. Prussin, Nucl. Inst. Methods 72, 125 (1969); J. T. Routti, Lawrence Radiation Laboratory Report No. UCRL-19452, 1969 (unpublished).

[22]D. C. Camp, Lawrence Radiation Laboratory Report No. UCRL-50156, 1967 (unpublished).

[23]M. Kanbe, M. Fujioka, and K. Histake, Nucl. Phys. A192, 151 (1972).

[24]R. S. Hager and E. C. Seltzer, Nucl. Data A4, 1 (1968).

[25]L. A. Sliv and I. M. Band, in Alpha-, Beta-, and Gamma-Ray Spectroscopy, edited by K. Siegbhan (North-Holland, Amsterdam, 1965).

[26]S. A. Moszkowski, Phys. Rev. 82, 35 (1951).

[27]J. F. Ziegler and G. A. Peterson, Phys. Rev. 165, 1337 (1968).

[28]K. K. Seth and P. D. Miller, to be published.

[29]T. T. S. Kuo and G. E. Brown, Nucl. Phys. 85, 40 (1966).

[30]The computer program used in these calculations was provided by Dr. James Vary.

[31]K. H. Maier, K. Nakai, R. M. Diamond, and F. S. Stephens, UCRL Report No. UCRL-19530, 1969 (unpublished), p. 40.

[32]K. Harada and S. Pittel, Phys. Letters 32B, 542 (1970).

[33]K. Harada and S. Pittel, Nucl. Phys. A159, 209 (1970).

[34]J. D. Vergados, Phys. Letters 36B, 12 (1971).

[35]J. C. Manthuruthil, C. P. Poirier, K. S. R. Sastry, R. F. Petry, B. K. Cantrell, and R. G. Wilkinson, Phys. Rev. C 4, 960 (1971).

[36]J. H. Hamilton, V. Ananthakrishnan, A. V. Ramayya, W. M. LaCasse, D. C. Camp, J. J. Pinajian, L. H. Kern, and J. C. Manthuruthil, Phys. Rev. (to be published).

[37]C. Ma and W. W. True, to be published.